ISSN 1674-1056
http://cpb.iphy.ac.cn
http://iopscience.iop.org/cpb
中国物理 B
Chinese Physics
中国物理
Chinese Physics B

Dynamical control of population and entanglement for open Λ-type atoms by engineering the environment

Xiao-Lan Wang(王晓岚), Yu-Kun Ren(任玉坤), Hao-Sheng Zeng(曾浩生)

Citation: Chin. Phys. B . 2019, 28(3): 030301. **doi:** 10.1088/1674-1056/28/3/030301
Journal homepage: http://cpb.iphy.ac.cn; http://iopscience.iop.org/cpb

What follows is a list of articles you may be interested in

Finite-size analysis of continuous-variable quantum key distribution with entanglement in the middle

Ying Guo(郭迎), Yu Su(苏玉), Jian Zhou(周健), Ling Zhang(张玲), Duan Huang(黄端)
Chin. Phys. B . 2019, 28(1): 010305. **doi:** 10.1088/1674-1056/28/1/010305

Noiseless linear amplification for the single-photon entanglement of arbitrary polarization-time-bin qudit

Ling-Quan Chen(陈灵泉), Yu-Bo Sheng(盛宇波), Lan Zhou(周澜)
Chin. Phys. B . 2019, 28(1): 010302. **doi:** 10.1088/1674-1056/28/1/010302

The entanglement of deterministic aperiodic quantum walks

Ting-Ting Liu(刘婷婷), Ya-Yun Hu(胡亚运), Jing Zhao(赵静), Ming Zhong(钟鸣), Pei-Qing Tong(童培庆)
Chin. Phys. B . 2018, 27(12): 120305. **doi:** 10.1088/1674-1056/27/12/120305

A new class of states of reversible entanglement manipulation under positive partial transpose operations

Jing Duan(段静), Yu Luo(罗宇), Yong-Ming Li(李永明)
Chin. Phys. B . 2018, 27(11): 110305. **doi:** 10.1088/1674-1056/27/11/110305

Population dynamics of excited atoms in non-Markovian environments at zero and finite temperature

Zou Hong-Mei, Fang Mao-Fa
Chin. Phys. B . 2015, 24(8): 080304. **doi:** 10.1088/1674-1056/24/8/080304

Dynamical control of population and entanglement for open Λ-type atoms by engineering the environment*

Xiao-Lan Wang(王晓岚), Yu-Kun Ren(任玉坤), and Hao-Sheng Zeng(曾浩生)†

Key Laboratory of Low-Dimensional Quantum Structures and Quantum Control of Ministry of Education, and Department of Physics, Hunan Normal University, Changsha 410081, *China*

(Received 6 September 2018; revised manuscript received 10 December 2018; published online 23 January 2019)

The exactly analytical solution for the dynamics of the dissipative Λ-type atom in the zero-temperature Lorentzian environment is presented. On this basis, we study the evolution of the population and entanglement. We find that the stable populations on the two lower levels of the Λ-type atom can be effectively adjusted by the combination of the relative decay rate and the environmental spectral frequency. However, for the initial Werner-like state, the stable entanglement between the two Λ-type atoms has very little tunability. Furthermore, the stable entanglement for the bilateral environment case is larger than that of the unilateral environmental case. A nonintuitive relation between the stable entanglement and stable population is found.

Keywords: open quantum systems, population, entanglement

PACS: 03.65.Ta, 03.65.Yz, 42.50.Lc **DOI:** 10.1088/1674-1056/28/3/030301

1. Introduction

The dynamics of open quantum systems is very sophisticated. Early study of these dynamics involved the application of the Born–Markov approximation, that is, neglecting all the memory effects, which led to the well-known Lindblad master equation.[1,2] The corresponding dynamics is attributed to the quantum Markovian processes. However, quantum non-Markovian processes are more realistic in principle. Many relevant physical systems, such as the quantum optical system,[3] the nanoscale solid-state quantum system,[4,5] quantum chemistry,[6] and the excitation transfer in the biological system,[7] should be treated by quantum non-Markovian processes. Recently, quantum non-Markovian processes have been studied extensively, from the measure of non-Markovianity of the processes[8–18] to the properties[19–29] and applications[30–37] of the dynamical processes.

The research of quantum non-Markovian processes is very much in favor of exact dynamics study because any approximation can possibly wipe out the memory effects. Due to this reason, the problem of a two-level atom dissipating in the zero-temperature environment becomes the paradigm for the investigation of non-Markovian processes, while the dissipative multilevel systems are relatively seldom involved. For the dynamics of V-type atoms dissipating in zero-temperature environments, the method of finding an exact solution has been discussed.[38,39] For the dissipative dynamics of Λ-type atoms, however, we have not yet found the relevant discussions, even though it has been touched on already.[40] One motivation of this paper is to present the exactly analytical solution for a three-level Λ-type atom dissipating in a zero-temperature Lorentzian environment.

The control of population and entanglement in multilevel quantum systems is very important for quantum information processing. In the ideal situation, the population transfer could be realized by optical pumping techniques.[41,42] For open quantum multilevel systems, it could be realized through the stimulated Raman adiabatic method.[43,44] There were many studies on the control of entanglement in dissipative environments, but most of them focused on qubit systems.[45–49] Although a few studies have involved the evolution of entanglement of dissipative V-type atoms,[50,51] similar research for the dissipative Λ-type atoms, without Born–Markov approximation, have not been reported yet. In this paper, based on the exact solution of the open Λ-type atom, we investigate the control of population and entanglement through the engineering of the decay rate and environmental spectral frequency.

The paper is organized as follows. In Section 2, we introduce the microscopic model for a Λ-type three-level atom interacting with a zero-temperature Lorentzian environment, and present the exact analytical solution. In Section 3, we study the problem of controlling population and entanglement. Finally, we give conclusions in Section 4.

2. Dynamical model and its solution

Our model is constituted by a Λ-type three-level atom embedded in an optical vacuum cavity with decay rate λ (Fig. 1(a)). The dissipative optical vacuum cavity can be described equivalently by a zero-temperature Lorentzian envi-

*Project supported by the National Natural Science Foundation of China (Grant No. 11275064), the Specialized Research Fund for the Doctoral Program of Higher Education, China (Grant No. 20124306110003), and the Construct Program of the National Key Discipline, China.

†Corresponding author. E-mail: hszeng@hunnu.edu.cn

© 2019 Chinese Physical Society and IOP Publishing Ltd

ronment that is a bosonic reservoir with infinite quantum harmonic oscillators. The configuration of energy levels of the Λ-type atom is depicted in Fig. 1(b), where $|1\rangle$, $|2\rangle$, and $|3\rangle$ denote the ground, meta-stable, and excited states, respectively. The transition frequencies from level $|3\rangle$ to levels $|1\rangle$ and $|2\rangle$ are denoted by ω_1 and ω_2, respectively, while the transition between $|2\rangle$ and $|1\rangle$ is forbidden. The Hamiltonian for the whole system may be written as

$$\begin{aligned} H &= -\omega_1|1\rangle\langle 1| - \omega_2|2\rangle\langle 2| + \sum_k \omega_k b_k^\dagger b_k \\ &\quad + \sum_k [g_{1k} b_k |3\rangle\langle 1| + g_{2k} b_k |3\rangle\langle 2| + \text{h.c.}], \end{aligned} \tag{1}$$

where b_k, $b_k^\dagger$, and ω_k are the annihilation, creation operators, and frequency for the k-th harmonic oscillator of the reservoir, with g_{1k} and g_{2k} being the coupling strengths between the reservoir and the two transition channels. In the above Hamiltonian, we have set the energy of level $|3\rangle$ to be zero and $\hbar = 1$.

Suppose that the atom is initially in a general pure state, so that the state of the compound system is

$$|\Psi(0)\rangle = [c_1(0)|1\rangle + c_2(0)|2\rangle + c_3(0)|3\rangle] \otimes |0\rangle_{\text{R}}, \tag{2}$$

where $|0\rangle_{\text{R}}$ denotes the vacuum state of the reservoir. The evolved state at any time t may be written as

$$\begin{aligned} |\Psi(t)\rangle &= [c_1(t)|1\rangle + c_2(t)|2\rangle + c_3(t)|3\rangle] \otimes |0\rangle_{\text{R}} \\ &\quad + \sum_k c_k(t)|1\rangle \otimes |1_k\rangle_{\text{R}} + \sum_k d_k(t)|2\rangle \otimes |1_k\rangle_{\text{R}}, \end{aligned} \tag{3}$$

where $|1_k\rangle_{\text{R}}$ indicates that there is one photon in the k-th mode of the reservoir, and all other modes are empty. Tracing over the environmental degrees of freedom, one obtains the reduced state of the atom in its natural bases as

$$\rho_{\text{s}}(t) = \begin{bmatrix} |c_1(t)|^2 + \sum_k |c_k(t)|^2 & c_1(t)c_2^*(t) + \sum_k c_k(t)d_k^*(t) & c_1(t)c_3^*(t) \\ c_2(t)c_1^*(t) + \sum_k d_k(t)c_k^*(t) & |c_2(t)|^2 + \sum_k |d_k(t)|^2 & c_2(t)c_3^*(t) \\ c_3(t)c_1^*(t) & c_3(t)c_2^*(t) & |c_3(t)|^2 \end{bmatrix}. \tag{4}$$

Here the evolution of the coefficients is determined by the following set of equations:

$$\dot{\text{i}}c_1(t) = -\omega_1 c_1(t), \tag{5a}$$

$$\dot{\text{i}}c_2(t) = -\omega_2 c_2(t), \tag{5b}$$

$$\dot{\text{i}}c_3(t) = \sum_k g_{1k} c_k(t) + \sum_k g_{2k} d_k(t), \tag{5c}$$

$$\dot{\text{i}}\dot{c}_k(t) = -\omega_1 c_k(t) + \omega_k c_k(t) + g_{1k}^* c_3(t), \tag{5d}$$

$$\dot{\text{i}}\dot{d}_k(t) = -\omega_2 d_k(t) + \omega_k d_k(t) + g_{2k}^* c_3(t). \tag{5e}$$

The evolution of $c_1(t)$ and $c_2(t)$ can be easily obtained,

$$c_1(t) = c_1(0)\,\text{e}^{\text{i}\omega_1 t}, \tag{6a}$$

$$c_2(t) = c_2(0)\,\text{e}^{\text{i}\omega_2 t}. \tag{6b}$$

To obtain the other coefficients, we formally integrate Eqs. (5d) and (5e) in the condition of $c_k(0) = d_k(0) = 0$ and obtain

$$c_k(t) = -\text{i}\int_0^t \text{d}\tau g_{1k}^* c_3(\tau)\,\text{e}^{\text{i}(\omega_1-\omega_k)(t-\tau)}, \tag{7a}$$

$$d_k(t) = -\text{i}\int_0^t \text{d}\tau g_{2k}^* c_3(\tau)\,\text{e}^{\text{i}(\omega_2-\omega_k)(t-\tau)}. \tag{7b}$$

Plugging them into Eq. (5c), in the continuum limitation $\sum_k g_{ik} g_{jk} \to \int \text{d}\omega J_{ij}(\omega)$ $(i, j = 1, 2)$, we obtain

$$\dot{c}_3(t) = -\int_0^t \text{d}\tau [f_1(t-\tau) + f_2(t-\tau)] c_3(\tau), \tag{8}$$

where the correlation function is defined by $f_j(t-\tau) = \int \text{d}\omega J_{jj}(\omega)\,\text{e}^{\text{i}(\omega_j-\omega)(t-\tau)}$.

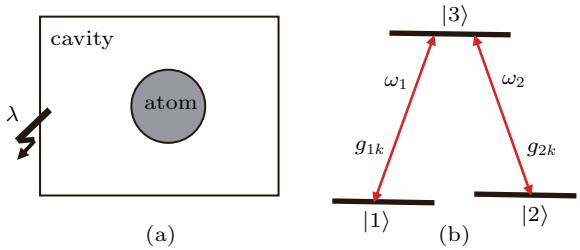


Fig. 1. (a) A Λ-type atom embedded in a vacuum cavity with decay rate λ; the latter may be described by a zero-temperature Lorentzian environment. (b) Energy levels of the Λ-type atom with ground, meta-stable, and excited states ($|1\rangle$, $|2\rangle$, and $|3\rangle$), respectively. The transitions $|1\rangle \leftrightarrow |3\rangle$ and $|2\rangle \leftrightarrow |3\rangle$ are allowed, but the transition between $|1\rangle$ and $|2\rangle$ is forbidden.

We use the Lorentzian distribution

$$J_{ij}(\omega) = \frac{1}{2\pi} \cdot \frac{\gamma_{ij}\lambda^2}{(\omega_0 - \omega)^2 + \lambda^2} \tag{9}$$

to describe the spectral density of the dissipative optical vacuum cavity. Here, ω_0 is the central frequency and the decay rate λ defines the spectral width. The parameter $\gamma_{jj} \equiv \gamma_j$ $(j = 1, 2)$ describes the spontaneous decay of level $|3\rangle$ to level $|j\rangle$, and γ_{ij} with $i \neq j$ describes the correlation between the two transitions. When the dipole moments of the two transitions are parallel, the relation $\gamma_{12} = \gamma_{21} = \sqrt{\gamma_1\gamma_2}$ is satisfied. In this paper, we consider only this case.

Under the condition of the Lorentzian spectrum, the correlation function becomes $f_j(t-\tau) = \frac{\gamma_j\lambda}{2}\,\text{e}^{-M_j(t-\tau)}$ with $M_j = \lambda + \text{i}(\omega_0 - \omega_j)$, and the solution of Eq. (8) may be written as

$$c_3(t) = \xi(t) c_3(0), \tag{10}$$

with $\xi(t)=(D_1\,\mathrm{e}^{b_1 t}+D_2\,\mathrm{e}^{b_2 t}+D_3\,\mathrm{e}^{b_3 t})$. Here, b_i are the roots of equation

$$R(p) = p^3+(M_1+M_2)p^2+\left(M_1M_2+\frac{\gamma_1\lambda}{2}+\frac{\gamma_2\lambda}{2}\right)p + \frac{\gamma_1\lambda}{2}M_2+\frac{\gamma_2\lambda}{2}M_1=0,$$

which are assumed non-degenerate. Since the degenerative probability is very small and can always be avoided by adjusting the structure parameters, we no longer consider the case here. The coefficients D_i are given by

$$D_i=\frac{(b_i+M_1)(b_i+M_2)}{3b_i^2+2(M_1+M_2)b_i+M_1M_2+\frac{\gamma_1\lambda}{2}+\frac{\gamma_2\lambda}{2}}. \tag{11}$$

Having $c_3(t)$ in hand, we can then obtain the evolution of $c_k(t)$ and $d_k(t)$. Equations (7a) and (7b), in transition to the continuum limitation, lead to

$$\sum_k|c_k(t)|^2 = \int_0^t\mathrm{d}\tau\int_0^t\mathrm{d}\tau' f_1(\tau'-\tau)c_3(\tau)c_3^*(\tau'), \tag{12}$$

$$\sum_k|d_k(t)|^2 = \int_0^t\mathrm{d}\tau\int_0^t\mathrm{d}\tau' f_2(\tau'-\tau)c_3(\tau)c_3^*(\tau'), \tag{13}$$

$$\begin{aligned}\sum_k c_k(t)d_k^*(t) &= \int_0^t\mathrm{d}\tau\int_0^t\mathrm{d}\tau'\int\mathrm{d}\omega J_{12}(\omega)\,\mathrm{e}^{\mathrm{i}\omega(\tau-\tau')}\\ &\quad\times\mathrm{e}^{\mathrm{i}(\omega_1 t-\omega_2 t-\omega_1\tau+\omega_2\tau')}c_3(\tau)c_3^*(\tau')\\ &= \frac{\gamma_{12}\lambda}{2}\mathrm{e}^{\mathrm{i}(\omega_1-\omega_2)t}\int_0^t\mathrm{d}\tau\int_0^t\mathrm{d}\tau' c_3(\tau)c_3^*(\tau')\\ &\quad\times\mathrm{e}^{-\lambda|\tau'-\tau|+\mathrm{i}(\delta_1\tau-\delta_2\tau')},\end{aligned} \tag{14}$$

where

$$\begin{aligned}f_j(\tau'-\tau) &= \int\mathrm{d}\omega J_{jj}(\omega)\exp[\mathrm{i}(\omega_j-\omega)(\tau'-\tau)]\\ &= \frac{\gamma_j\lambda}{2}\exp[-\lambda|\tau'-\tau|-\mathrm{i}\delta_j(\tau'-\tau)],\end{aligned}$$

$\delta_j=\omega_0-\omega_j$, and we use

$$\int\mathrm{d}\omega J_{12}(\omega)\,\mathrm{e}^{\mathrm{i}\omega(\tau-\tau')}=\frac{\gamma_{12}\lambda}{2}\,\mathrm{e}^{-\lambda|\tau'-\tau|-\mathrm{i}\omega_0(\tau'-\tau)}$$

in the second equality of Eq. (14).

The double integrals in Eqs. (12)–(14) can be solved further. Using

$$|\tau'-\tau|=\begin{cases}\tau'-\tau, & \text{if}\quad \tau'\geq\tau,\\ \tau-\tau', & \text{if}\quad \tau'<\tau\end{cases}$$

to divide the integral with respect to τ' into two parts, after tedious but straightforward calculation, we finally obtain

$$\sum_k|c_k(t)|^2=\alpha_1(t)|c_3(0)|^2, \tag{15a}$$

$$\sum_k|d_k(t)|^2=\alpha_2(t)|c_3(0)|^2, \tag{15b}$$

$$\sum_k c_k(t)d_k^*(t)=\Theta(t)|c_3(0)|^2, \tag{15c}$$

where

$$\begin{aligned}\alpha_1(t) &= \frac{\gamma_1\lambda}{2}\sum_{j,l=1}^{3}D_jD_l^*\{\Omega_1^{jl}\,\mathrm{e}^{(b_j+b_l^*)t}+\Omega_2^{jl}\,\mathrm{e}^{(-\lambda+b_j+\mathrm{i}\delta_1)t}\\ &\quad+\Omega_3^{jl}\,\mathrm{e}^{(-\lambda+b_l^*-\mathrm{i}\delta_1)t}+\Omega_4^{jl}\},\end{aligned} \tag{16}$$

$$\begin{aligned}\Theta(t) &= \frac{\gamma_{12}\lambda}{2}\sum_{j,l=1}^{3}D_jD_l^*\{W_1^{jl}\,\mathrm{e}^{(b_j+b_l^*)t}+W_2^{jl}\,\mathrm{e}^{(-\lambda+b_j+\mathrm{i}\delta_2)t}\\ &\quad+W_3^{jl}\,\mathrm{e}^{(-\lambda+b_l^*-\mathrm{i}\delta_1)t}+W_4^{jl}\,\mathrm{e}^{\mathrm{i}(\omega_1-\omega_2)t}\},\end{aligned} \tag{17}$$

with

$$\begin{aligned}\Omega_1^{jl} &= \frac{1}{(-\lambda+b_l^*-\mathrm{i}\delta_1)(\lambda+b_j+\mathrm{i}\delta_1)}\\ &\quad-\frac{2\lambda}{(\lambda+b_l^*-\mathrm{i}\delta_1)(-\lambda+b_l^*-\mathrm{i}\delta_1)(b_j+b_l^*)},\\ \Omega_2^{jl} &= \frac{1}{(\lambda-b_j-\mathrm{i}\delta_1)(\lambda+b_l^*-\mathrm{i}\delta_1)},\\ W_1^{jl} &= \frac{1}{(-\lambda+b_l^*-\mathrm{i}\delta_2)(\lambda+b_j+\mathrm{i}\delta_1)}\\ &\quad-\frac{2\lambda}{(\lambda+b_l^*-\mathrm{i}\delta_2)(-\lambda+b_l^*-\mathrm{i}\delta_2)[b_j+b_l^*+\mathrm{i}(\omega_2-\omega_1)]},\\ W_2^{jl} &= \frac{1}{(\lambda+b_l^*-\mathrm{i}\delta_2)(\lambda-b_j-\mathrm{i}\delta_1)}.\end{aligned}$$

The other four coefficients can be obtained through the following replacement:

$$\Omega_1^{jl}\ \xrightarrow{\lambda\to-\lambda}\ \Omega_4^{jl},\quad \Omega_2^{jl}\ \xrightarrow{\lambda\to-\lambda}\ \Omega_3^{jl},$$

$$W_1^{jl}\ \xrightarrow{\lambda\to-\lambda}\ W_4^{jl},\quad W_2^{jl}\ \xrightarrow{\lambda\to-\lambda}\ W_3^{jl}.$$

In addition, the coefficient $\alpha_2(t)$ in Eq. (15b) can be obtained by making the replacement

$$\alpha_1(t)\ \xrightarrow{\gamma_1\to\gamma_2,\,\omega_1\to\omega_2}\ \alpha_2(t). \tag{18}$$

Finally, the reduced density matrix equation (4) can be written as

$$\rho_{\mathrm{s}}(t)=\begin{bmatrix}P_1(t) & \rho_{12}(t) & \rho_{13}(t)\\ \rho_{12}^*(t) & P_2(t) & \rho_{23}(t)\\ \rho_{13}^*(t) & \rho_{23}^*(t) & P_3(t)\end{bmatrix}, \tag{19}$$

where $\rho_{12}(t)=c_1(0)c_2^*(0)\,\mathrm{e}^{\mathrm{i}(\omega_1-\omega_2)t}+\Theta(t)|c_3(0)|^2$, $\rho_{13}(t)=T_1(t)c_1(0)c_3^*(0)$, $\rho_{23}(t)=T_2(t)c_2(0)c_3^*(0)$ with

$$T_1(t) = \mathrm{e}^{\mathrm{i}\omega_1 t}\left(\sum_{j=1}^{3}D_j^*\,\mathrm{e}^{b_j^* t}\right),$$

$$T_2(t) = \mathrm{e}^{\mathrm{i}\omega_2 t}\left(\sum_{j=1}^{3}D_j^*\,\mathrm{e}^{b_j^* t}\right).$$

The populations of the three levels of the Λ-type atom are, respectively,

$$P_j(t)=|c_j(0)|^2+\alpha_j(t)|c_3(0)|^2,\quad j=1,2, \tag{20}$$

$$P_3=|\xi(t)|^2|c_3(0)|^2. \tag{21}$$

From Eq. (19), we can easily obtain the quantum map ε for the dynamics of the open Λ-type atom

$$\begin{aligned}
\varepsilon(|1\rangle\langle 1|) &= |1\rangle\langle 1|,\\
\varepsilon(|2\rangle\langle 2|) &= |2\rangle\langle 2|,\\
\varepsilon(|3\rangle\langle 3|) &= \alpha_1(t)|1\rangle\langle 1|+\alpha_2(t)|2\rangle\langle 2|+\alpha_3(t)|3\rangle\langle 3|\\
&\quad +\Theta(t)|1\rangle\langle 2|+\Theta^*(t)|2\rangle\langle 1|,\\
\varepsilon(|1\rangle\langle 2|) &= \exp[\mathrm{i}(\omega_1-\omega_2)t]|1\rangle\langle 2|,\\
\varepsilon(|1\rangle\langle 3|) &= |1\rangle\langle 3|,\\
\varepsilon(|2\rangle\langle 3|) &= |2\rangle\langle 3|,
\end{aligned} \tag{22}$$

which will be used in the study of entanglement evolution.

3. Control of population and entanglement

To study the evolution of population, we assume that the atom initially populates in the excited level $|3\rangle$, i.e., initially the atomic state is given by Eq. (2) with $c_1(0)=c_2(0)=0$ and $c_3(0)=1$. In Fig. 2(a), we show the evolution of the three populations over dimensionless time for $\gamma_1=\gamma_2=\gamma$. As expected, the excited population P_3 decays monotonically and the populations $P_{1,2}$ increase continuously. To avoid overlap of curves, we set the spectral frequency to be $\omega_0=84\gamma$, which deviates slightly from the central frequency 85γ between ω_1 and ω_2, leading to a quicker increase in P_2 (red line) than P_1 (blue line). This result implies that the stable populations of levels $|1\rangle$ and $|2\rangle$ should be related to both the spectral frequency ω_0 and the decay rates $\gamma_{1,2}$.

In Fig. 2(b), we show the evolution of the stable populations of the three levels versus the relative decay rate γ_2/γ_1 for $\gamma t=50$, where the spectral frequency ω_0 is set to be the center between ω_1 and ω_2. It is shown that in the stable state, the population P_3 of the excited level is zero, and P_1 decreases and P_2 increases with the change of γ_2/γ_1. The intersection of the two curves corresponds to $P_1=P_2=0.5$ and $\gamma_2/\gamma_1=1$. Figure 2(b) tells us that if the relative decay rate γ_2/γ_1 can be adjusted, we can then control the stable populations of levels $|1\rangle$ and $|2\rangle$.

In Fig. 2(c), we show the evolution of the stable populations versus the spectral frequency ω_0/γ. It is shown that, in the case of $\gamma_2=\gamma_1$, when ω_0 resonates approximately with ω_2, the stable population P_2 approaches one and P_1 approaches zero, and the result exchanges when ω_0 approaches ω_1 (see the dash lines). However in the case that the difference between γ_1 and γ_2 is large ($\gamma_2=9\gamma_1$ for the solid lines in the figure), the situation is different: when ω_0 approaches ω_2, the stable value of P_2 is more close to one and P_1 is more close to zero; but when ω_0 approaches ω_1, although the stable value of P_1 is larger than P_2, they are far away from one or zero. This is the result of the cooperative effect between resonance and decay: both a large decay rate and resonance can improve the stable population. When ω_0 resonates with ω_2, the cooperative effect is constructive, i.e., both resonance and decay improve the stable value of P_2; when ω_0 approaches ω_1, the cooperative effect is destructive, i.e., the resonant effect improves but the smaller γ_1 reduces the stable value of P_1. These results remind us that we should use the combination of spectral frequency and decay rates to control stable populations.

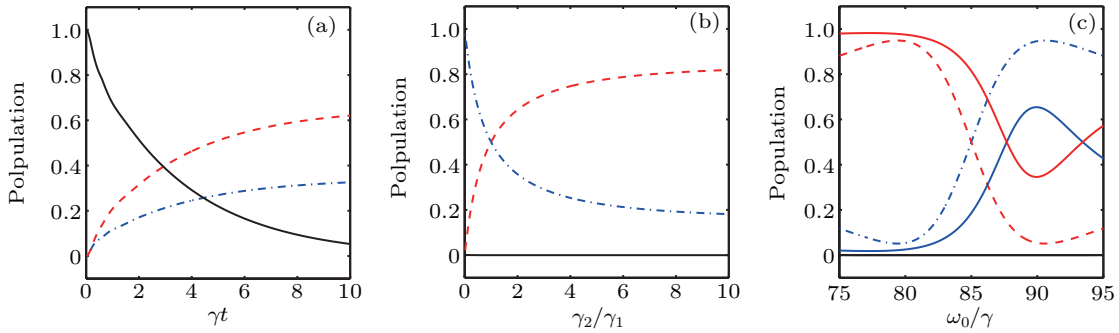


Fig. 2. Population versus (a) dimensionless time γt, (b) relative decay rate γ_2/γ_1, and (c) spectral frequency ω_0/γ for the initial state given by Eq. (2) with $c_1(0)=c_2(0)=0$ and $c_3(0)=1$. The blue, red, and black lines correspond to populations P_1, P_2, and P_3, respectively. Other parameters are set as $\gamma_1=\gamma$, $\lambda=2\gamma$, $\omega_1=90\gamma$, and $\omega_2=80\gamma$. (a) $\gamma_2=\gamma$, $\omega_0=84\gamma$; (b) $\gamma t=50$, $\omega_0=85\gamma$; (c) $\gamma t=50$, $\gamma_2=\gamma$ (dash lines) or $\gamma_2=9\gamma$ (solid lines).

To study the evolution of entanglement, we employ the notion of entanglement negativity. For a bipartite system state ρ_{AB}, the entanglement negativity is defined as[52,53]

$$N(\rho_{\mathrm{AB}})=\sum_k|\eta_k^{T_{\mathrm{A}}(-)}|=\frac{\sum_k|\eta_k^{T_{\mathrm{A}}}|-1}{2}, \tag{23}$$

where $\eta_k^{T_{\mathrm{A}}(-)}$ and $\eta_k^{T_{\mathrm{A}}}$ are, respectively, the negative and all eigenvalues of the partial transpose of ρ_{AB} with respect to subsystem A.

Having Eq. (22) in hand, we can calculate in principle the evolution of any quantum entangled state. Here we take the Werner-like state[54]

$$\rho_\varepsilon=\frac{(1-\varepsilon)}{9}I+\varepsilon|\Psi^{\mathrm{AB}}\rangle\langle\Psi^{\mathrm{AB}}| \tag{24}$$

as the exemplary example. Here, I denotes the three-dimensional identity matrix, and $|\Psi^{\mathrm{AB}}\rangle=\frac{1}{\sqrt{3}}(|11\rangle+|22\rangle+$

$|33\rangle$) is a maximally entangled state of two qutrits A and B. The Werner-like state is separable for $0 \leq \varepsilon \leq 1/4$, and entangled for $1/4 < \varepsilon \leq 1$.

We discuss the problem in two cases: the unilateral environment and the bilateral environment. The former means that only atom A is influenced by the noisy environment while atom B remains noise-free; the later means that both atoms are influenced by noises. In Fig. 3, we show the time evolution of the entanglement negativity of the Werner-like state for these two cases. It is shown that the entanglement negativity has similar decay behaviors for the unilateral and bilateral environments: after the decaying at the initial stage, the entanglement negativity reaches a stable value that depends on the parameter ε. The difference between the unilateral and bilateral environments is mainly reflected in three aspects. 1) In the initial stage, the entanglement for the bilateral environment case reduces faster than that for the unilateral environment case. 2) The stable entanglement for the bilateral environment case is larger than that for the unilateral environment case. 3) The entanglement for the bilateral environment case has a momentary restoration after decaying in the initial stage. The first difference is intuitive, because the bilateral environment has a larger noisy effect than the unilateral environment. The second difference may be explained as follows. The stable entanglement for the unilateral environment case is formed between an effective two-level system and a three-level system, but for the bilateral environment case it is formed between two effective two-level systems. When the populations of the excited levels of both entangled Λ-type atoms decay into their lower levels, there is more entanglement. Finally, the momentary restoration of entanglement for the bilateral environment case implies that there are some intermediate states in the decay process, which have less entanglement than the stable state.

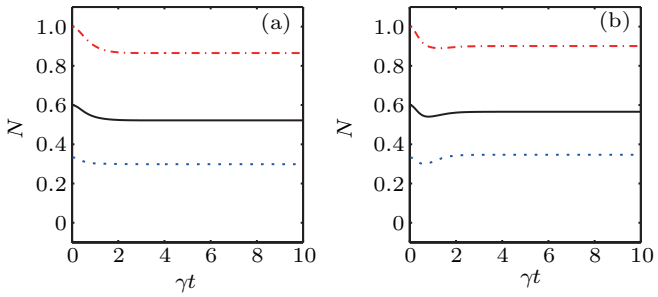


Fig. 3. Evolution of entanglement versus dimensionless time γt for the Werner-like state with $\varepsilon = 1$ (dot-dash red lines), $\varepsilon = 0.7$ (solid black lines), and $\varepsilon = 0.5$ (dash blue lines): (a) bilateral environment case and (b) unilateral environment case. The parameters are chosen as $\gamma_1 = \gamma_2 = \gamma$, $\lambda = 2\gamma$, $\omega_1 = 92\gamma$, $\omega_2 = 90\gamma$, and $\omega_0 = 91\gamma$.

In Fig. 4, we show the evolution of the stable entanglement versus the relative decay rate γ_2/γ_1 for the unilateral and bilateral environments. It is shown that the stable entanglement for the unilateral environment case almost remains unchanged, and only has some tiny changes in the beginning stage of γ_2/γ_1 for the bilateral environment case. This is sharply contrasted with the decaying of populations where the stable populations $P_{1,2}$ change remarkably with γ_2/γ_1. In addition, it is seen more clearly that the stable entanglement for the bilateral environment case is lager than that for the unilateral environment case, which agrees with the result presented by Fig. 3.

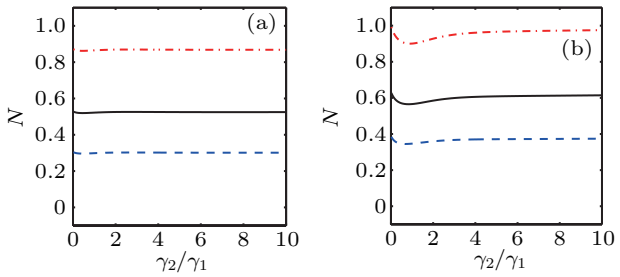


Fig. 4. Asymptotic entanglement versus relative decay rate γ_2/γ_1 for the Werner-like state with $\varepsilon = 1$ (dot-dash red lines), $\varepsilon = 0.7$ (solid black lines), and $\varepsilon = 0.5$ (dash blue lines): (a) bilateral environment case and (b) unilateral environment case. Here, $\gamma_1 = \gamma$, $\lambda = 2\gamma$, $\omega_1 = 92\gamma$, $\omega_2 = 90\gamma$, $\omega_0 = 91\gamma$, and $\gamma t = 50$.

Figure 5 shows the evolution of stable entanglement versus the environmental spectral frequency for the Werner-like state with $\varepsilon = 1$, i.e., the maximally entangled state $|\Psi^{\mathrm{AB}}\rangle$. It again shows that the stable entanglement for the bilateral environment case is lager than that for the unilateral environment case. For the unilateral environment, the stable entanglement is almost unchanged when ω_0/γ changes (lower dash lines). For the bilateral environment, it also has limited adjustability via the change in ω_0 (upper solid lines). The minimum stable entanglement for the case of $\gamma_1 = \gamma_2$ takes place at $\omega_0/\gamma = 85$, i.e., at the center between ω_1 and ω_2 (red lines). For $\gamma_2 = 9\gamma_1$, the minimum points move to the right (blue lines). The results of Figs. 4 and 5 imply that the stable entanglement for the open Λ-type atoms has only little adjustability by engineering the environmental spectral frequency and the relative decay rate.

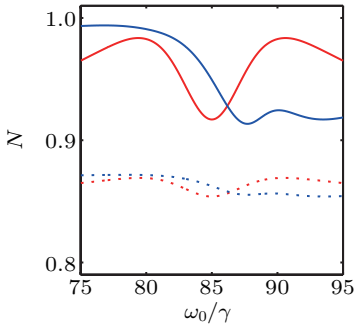


Fig. 5. Asymptotic entanglement versus dimensionless frequency ω_0/γ for the Werner-like state with $\varepsilon = 1$, where $\omega_1 = 90\gamma$, $\omega_2 = 80\gamma$, $\lambda = 2\gamma$, and $\gamma t = 50$. Red lines correspond to $\gamma_1 = \gamma_2 = \gamma$ and blue lines correspond to $\gamma_1 = \gamma$, $\gamma_2 = 9\gamma$. The upper solid lines correspond to the bilateral environment and the lower dash lines correspond to the unilateral environment.

There is a nonintuitive result that needs to be mentioned. For the initial Werner-like state, and in the conditions of $\gamma_1 = \gamma_2$ and $\omega_0 = (\omega_1 + \omega_2)/2$, the stable populations of each

atom should satisfy $P_1 = P_2$ (refer to Fig. 2(b)), where the corresponding stable entanglement is just the minimum (red lines in Fig. 5). On the contrary, when ω_0 resonates with ω_1 or ω_2, the stable populations $P_{1,2}$ have great disparity (dash lines in Fig. 2(c)), where the stable entanglement is the maximum (red lines in Fig. 5). In other words, the smaller the population difference, the smaller the entanglement. This result can also be seen from Fig. 4(b), where the stable entanglement has its minimum for $\gamma_2/\gamma_1 = 1$ (corresponding to $P_1 = P_2$), and increases when γ_2/γ_1 deviates from this point. This is sharply contrastive with the fact that a maximal entangled pure state, i.e., Bell state, has equal weight between the two levels.

4. Conclusion

We have presented the exact solution of the dynamics for an open Λ-type atom dissipating in the zero-temperature Lorentzian environment. Special attention has been paid to the study of the stable population and stable entanglement. We have found that the stable populations on the two lower levels of the Λ-type atom can be effectively adjusted by the combination of relative decay rate and environmental spectral frequency. Both a large decay rate and resonance effect between the atomic transition and environmental frequency can improve the stable population.

In the discussion of entanglement, we have distinguished two cases of unilateral and bilateral environments. We have found that the entanglement for the bilateral environment case decays faster but its stable value is larger than that of the unilateral environment case. Unlike the evolution of populations, the stable entanglement for both unilateral and bilateral environments only has very restrictive adjustability by engineering the decay rates or environmental spectral frequency. A nonintuitive relation between the stable entanglement and stable population has been found: the smaller the population difference between the two lower levels of the Λ-type atom, the smaller the entanglement.

References

[1] Lindblad G 1976 *Commun. Math. Phys.* **48** 119
[2] Gorini V, Kossakowski A and Sudarshan E C G 1976 *J. Math. Phys.* **17** 821
[3] Breuer H P and Petruccione F 2002 *The Theory of Open Quantum Systems* (Oxford: Oxford University Press)
[4] Buluta I, Ashhab S and Nori F 2011 *Rep. Prog. Phys.* **74** 104401
[5] You J Q and Nori F 2005 *Phys. Today* **58** 42
[6] Shao J 2004 *J. Chem. Phys.* **120** 5053
[7] Chin A W, Datta A, Caruso F, Huelga S F and Plenio M B 2010 *New J. Phys.* **12** 065002
[8] Breuer H P, Laine E M and Piilo J 2009 *Phys. Rev. Lett.* **103** 210401
[9] Rivas Á, Huelga S F and Plenio M B 2010 *Phys. Rev. Lett.* **105** 050403
[10] Lu X M, Wang X G and Sun C P 2010 *Phys. Rev. A* **82** 042103
[11] Luo S, Fu S and Song H 2012 *Phys. Rev. A* **86** 044101
[12] Chruscinski D and Maniscalco S 2014 *Phys. Rev. Lett.* **112** 120404
[13] Chruscinski D, Macchiavello C and Maniscalco S 2017 *Phys. Rev. Lett.* **118** 080404
[14] Song H, Luo S and Hong Y 2015 *Phys. Rev. A* **91** 042110
[15] Chen S L, Lambert N, Li C M, Miranowicz A, Chen Y N and Nori F 2016 *Phys. Rev. Lett.* **116** 020503
[16] Dhar H S, Bera M N and Adesso G 2015 *Phys. Rev. A* **91** 032115
[17] Paula F M, Obando P C and Sarandy M S 2016 *Phys. Rev. A* **93** 042337
[18] He Z, Zeng H S, Li Y, Wang Q and Yao C 2017 *Phys. Rev. A* **96** 022106
[19] Haikka P, Johnson T H and Maniscalco S 2013 *Phys. Rev. A* **87** 010103(R)
[20] Addis C, Brebner G, Haikka P and Maniscalco S 2014 *Phys. Rev. A* **89** 024101
[21] Zeng H S, Zheng Y P, Tang N and Wang G Y 2013 *Quantum Inf. Process* **12** 1637
[22] Wissmann S, Breuer H P and Vacchini B 2015 *Phys. Rev. A.* **92** 042108
[23] Bae J and Chruscinski D 2016 *Phys. Rev. Lett.* **117** 050403
[24] Bylicka B, Johansson M and Acin A 2017 *Phys. Rev. Lett.* **118** 120501
[25] Liu Y, Cheng W, Gao Z Y and Zeng H S 2015 *Opt. Express* **23** 023021
[26] Liu Y, Zou H M and Fang M F 2018 *Chin. Phys. B* **27** 010304
[27] Gao D Y, Gao Q and Xia Y J 2017 *Chin. Phys. B* **26** 110303
[28] Zou H M and Fang M F 2015 *Chin. Phys. B* **24** 080304
[29] Ding B F, Wang X Y, Tang Y F, Mi X W and Zhao H P 2011 *Chin. Phys. B* **20** 060304
[30] Chin A W, Huelga S F and Plenio M B 2012 *Phys. Rev. Lett.* **109** 233601
[31] Vasile R, Olivares S, Paris M G A and Maniscalco S 2011 *Phys. Rev. A* **83** 042321
[32] Laine E M, Breuer H P and Piilo J 2014 *Sci. Rep.* **4** 4620
[33] Bylicka B, Chruściński D and Maniscalco S 2014 *Sci. Rep.* **4** 5720
[34] Tang N, Fan Z L and Zeng H S 2015 *Quantum Inf. Comput.* **15** 0568
[35] Xu K, Han W, Zhang Y J and Fan H 2018 *Chin. Phys. B* **27** 010302
[36] He Z, Yao C M, Li L and Wang Q 2016 *Chin. Phys. B* **25** 080304
[37] Ren Y K, Wang X L and Zeng H S 2018 *Quantum Inf. Process* **17** 5
[38] Garraway B M 1997 *Phys. Rev. A.* **55** 2290
[39] Fan Z L, Ren Y K and Zeng H S 2016 *Chin. Phys. B* **25** 010303
[40] Gu W J and Li G X 2012 *Phys. Rev. A* **85** 014101
[41] Hamilton C H, Kinsey J L and Field R W 1986 *Annu. Rev. Phys. Chem.* **37** 493
[42] Meier W, Ahlers G and Zacharias H 1986 *J. Chem. Phys.* **85** 2599
[43] Scala M, Militello B, Messina A and Vitanov N V 2011 *Phys. Rev. A* **83** 012101
[44] Wang Q, Nie J J and Zeng H S 2013 *Eur. Phys. J. D* **67** 151
[45] Yu T and Eberly J H 2004 *Phys. Rev. Lett.* **93** 140404
[46] Bellomo B, Lo Franco R and Compagno G 2007 *Phys. Rev. Lett.* **99** 160502
[47] Bellomo B, Lo Franco R and Compagno G 2008 *Phys. Rev. A* **77** 032342
[48] Cao X and Zheng H 2008 *Phys. Rev. A* **77** 022320
[49] Golkar S and Tavassoly 2018 *Chin. Phys. B* **27** 040303
[50] Derkacz L and Jakobczyk 2006 *Phys. Rev. A* **74** 032313
[51] Checinska A and Wodkiewicz K 2007 *Phys. Rev. A.* **76** 052306
[52] Peres A 1996 *Phys. Rev. Lett.* **77** 1413
[53] Horodečki P 1997 *Phys. Lett. A* **232** 333
[54] Werner R F 1989 *Phys. Rev. A* **40** 4277